Nucleoside triphosphate pentose ring impact on CFTR gating and hydrolysis

Andrei A. Aleksandrov*, Luba Aleksandrov, John R. Riordan

Mayo Foundation and Mayo Clinic Scottsdale, S.C. Johnson Medical Research Center, 13400 E. Shea Blvd., Scottsdale, AZ 85259, USA

Received 20 March 2002; revised 4 April 2002; accepted 5 April 2002

First published online 16 April 2002

Edited by Maurice Montal

Abstract Alterations in the pentose ring of ATP have a major impact on cystic fibrosis transmembrane conductance regulator (CFTR) function. Both 2′- and 3′-deoxy-ATP (dATP) accelerate ion channel openings and stabilize open channel structure better than ATP. Purified wild-type CFTR hydrolyzes dATP. The apparent first-order rate constants for hydrolysis at low substrate concentration are the same for dATP and ATP. This suggests that product release and/or relaxation of the enzyme structure to the initial ligand free state is the rate-limiting step in the CFTR hydrolytic cycle. Circumvention of the normal requirement for protein kinase A phosphorylation of the R-domain for channel activation implies that the impact of the deoxyribonucleotide interaction with the nucleotide binding domains is transmitted to the channel-forming elements of the protein more readily than that of the ribonucleotide. © 2002 Published by Elsevier Science B.V. on behalf of the Federation of European Biochemical Societies.

Key words: Cystic fibrosis transmembrane conductance regulator; Gating kinetics; ATP hydrolysis

1. Introduction

Modification of the substrate structure is a widely used tool to investigate the relationship between structure and function of enzymes. Three major groups of nucleoside triphosphate analogs are typically used to investigate the specificity of nucleoside triphosphate converting enzymes: modifications in the nitrogenous heterocyclic base, modifications in the phosphate chain, and modifications in the pentose ring [1,2]. Until now, only the effect of the first two of these moieties have been tested on cystic fibrosis transmembrane conductance regulator (CFTR) ion channel gating [3–7].

The role of the pentose ring in the purine nucleoside moiety has received little attention. A brief abstract reports that 2′- (or 3′)-*O*-(trinitrophenyl)adenosine 5′-triphosphate is unable to stimulate CFTR ion channel current [8]. We have now focused on the hydroxyl groups at the 2′- and 3′-positions of the ring. Strikingly, either 2′- or 3′-deoxy-ATP (dATP) was found to gate protein kinase A (PKA) phosphorylated wild-type CFTR channels more effectively than ATP. Most remarkably it was found that dATP obviated the need for PKA phosphorylation for CFTR channel activation. Moreover, a PKA unresponsive mutant in which 15 sites of PKA phosphorylation in the R-domain were mutated [9] was activated by dATP. Although the means by which dATP circumvents the need for R-domain phosphorylation in CFTR channel activation has not been fully elucidated, a reduced K_M for hydrolysis by the purified protein was observed. The constant value of V_{max}/K_M for both ATP and dATP supports our earlier assumption that product dissociation and/or relaxation of the enzyme structure is the rate-limiting step for both ion channel closing and nucleotide triphosphate hydrolysis [10].

2. Materials and methods

2.1. Membrane vesicle treatment

Microsomal vesicles from Chinese hamster ovary cells stably expressing CFTR [11] were isolated as described before [10]. Vesicles were stored at −80°C. Directly before use they were thawed and phosphorylated by 100 U/ml PKA catalytic subunit and 0.5 mM Na_2ATP for 20 min at room temperature. Alkaline phosphatase (100 U/ml) was substituted for PKA and ATP to generate control vesicles with non-phosphorylated CFTR. After 30 min treatment at room temperature, alkaline phosphatase was washed out by pelleting the vesicles (1 h at $100\,000\times g$). The pellet was resuspended in prephosphorylation buffer and briefly sonicated for 3×20 s.

2.2. Single channel measurements

Single channel measurements were made as described previously [10]. Planar lipid bilayers were painted onto a 0.2 mm hole drilled in a Teflon cup using a phospholipid solution in *n*-decane containing a 2:1 mixture of 1-palmitoyl-2-oleoyl-*sn*-glycero-3-phosphoethanolamine and 1-palmitoyl-2-oleoyl-*sn*-glycero-3-phosphoserine (20 mg/ml). The lipid bilayer separated 1.0 ml of solution in the Teflon cup (*cis*-side) from 4.0 ml of a solution in an outer glass chamber (*trans*-side). Membrane vesicles were added as a concentrated stock solution to the *cis*-side with a final protein concentration of 10–15 μg/ml. Both chambers were magnetically stirred. Heating and temperature control were established by Temperature Control System TC2BIP (Cell MicroControls, Virginia Beach, VA, USA). Electrical contact between solutions was provided by Ag/AgCl electrodes through an agar bridge filled with 0.5 M KCl. The membrane potential difference was measured as a *cis*-side potential with the *trans*-side grounded. Electrical measurements of single channel current were performed under voltage clamp conditions using an Axopatch 200B amplifier (Axon Instruments, Foster City, CA, USA) after fusion of the membrane vesicles containing CFTR with the preformed lipid bilayer. The output signal was filtered with an eight-pole low pass Bessel filter LPBF-48DG (NPI Electronic, Germany) with a cut-off frequency of 50 Hz. For data analysis, the signal was digitized with a Digidata 1200 (Axon Instruments) at a sampling rate of 500 Hz and analyzed using pCLAMP 6.0 software (Axon Instruments). Origin 4.0 software (Microcal Software, Northhampton, MA, USA) was used to fit the all points histograms by multi-peak Gaussian curves. All measurements were done at 30°C in symmetrical salt solutions containing, in mM: 300 Tris–HCl, 3 $MgCl_2$, 1 EGTA, pH 7.2. The endogenous cation channels were invisible under these ionic conditions. With 2 mM ATP

*Corresponding author. Fax: (1)-480-301 7017.
E-mail address: aleksand@mayo.edu (A.A. Aleksandrov).

Abbreviations: CFTR, cystic fibrosis transmembrane conductance regulator; NBD, nucleotide binding domain; PKA, protein kinase A

0014-5793/02/$22.00
PII: S0014-5793(02)02698-4

added to the *cis*-side, CFTR ion channels appeared only after fusion of PKA phosphorylated inside-out vesicles. Experimental data for the analysis of gating kinetics were collected not less than 20 min after any change in experimental conditions.

2.3. CFTR purification and reconstitution

A crude membrane fraction was prepared from baby hamster kidney cells expressing CFTR-His_{10} by homogenizing cells in cold hypotonic buffer (10 mM HEPES, pH 7.2, 1 mM EDTA, protease inhibitor cocktail). Microsomes were collected by sedimentation of the post-nuclear supernatant ($600\times g$, 15 min) at $100\,000\times g$ for 30 min.

To remove peripheral proteins the crude membrane fraction was resuspended in 100 ml 40 mM Tris buffer, pH 10.8, and incubated for 20 min at 4°C. The alkali-stripped membranes were collected by centrifugation (pelleting) at $100\,000\times g$ for 30 min and then resuspended in 30 ml of solubilization buffer A (20 mM Tris–HCl, pH 7.4, 500 mM NaCl, 2 mM $MgCl_2$, 20% glycerol, 1% (w/v) *n*-dodecyl-β-D-maltoside (DDM) and 0.2% lipids (*Escherichia coli* crude lipids/PC = 3:1). After 40 min agitation the insoluble membrane fragments were pelleted by centrifugation at $100\,000\times g$ for 30 min. After addition of 5 mM imidazole the supernatant was mixed with Ni-NTA resin and incubated overnight at 4°C. The mixture was poured into a column and washed with 10 volumes of buffer B (20 mM Tris–HCl with pH 6.8, 500 mM NaCl, 2 mM $MgCl_2$, 20% glycerol) plus 60 mM imidazole and 1% DDM. To elute CFTR, the imidazole concentration was increased to 400 mM. The eluate was mixed with wheat germ lectin Sepharose 6 MB equilibrated in the same buffer. The mixture was shaken overnight at 4°C and washed with buffer B plus 1 mM dithiothreitol (DTT), 0.1% DDM and a lipid mixture (PE/PC/PS/cholesterol, 5:3:1:1). CFTR was eluted with buffer C containing 20 mM Tris–HCl (pH 9.0), 500 mM NaCl, 1 mM DTT, 50% ethylene glycol, 0.5 M *N*-acetylglucosamine, 0.1% DDM and the same lipid mixture. The eluate was dialyzed for 2 days against buffer D (20 mM Tris–HCl, pH 7.4, 100 mM NaCl and 2 mM $MgCl_2$).

2.4. Assay of ATPase activity

The ability of purified CFTR to hydrolyze ATP was assayed by measuring the formation of [α-^{32}P]ADP from [α-^{32}P]ATP. The reaction mixture containing buffer (40 mM Tris–HCl, pH 7.4, 1 mM DTT, 4 mM $MgCl_2$, 2 mM Na_2ATP, 1 μCi [α-^{32}P]ATP) and a sample of purified CFTR was incubated 90 min at 30°C. An aliquot was spotted onto a polyethyleneimine–cellulose thin layer plate and developed in 0.5 M LiCl plus 1 M formic acid. The plate was dried and

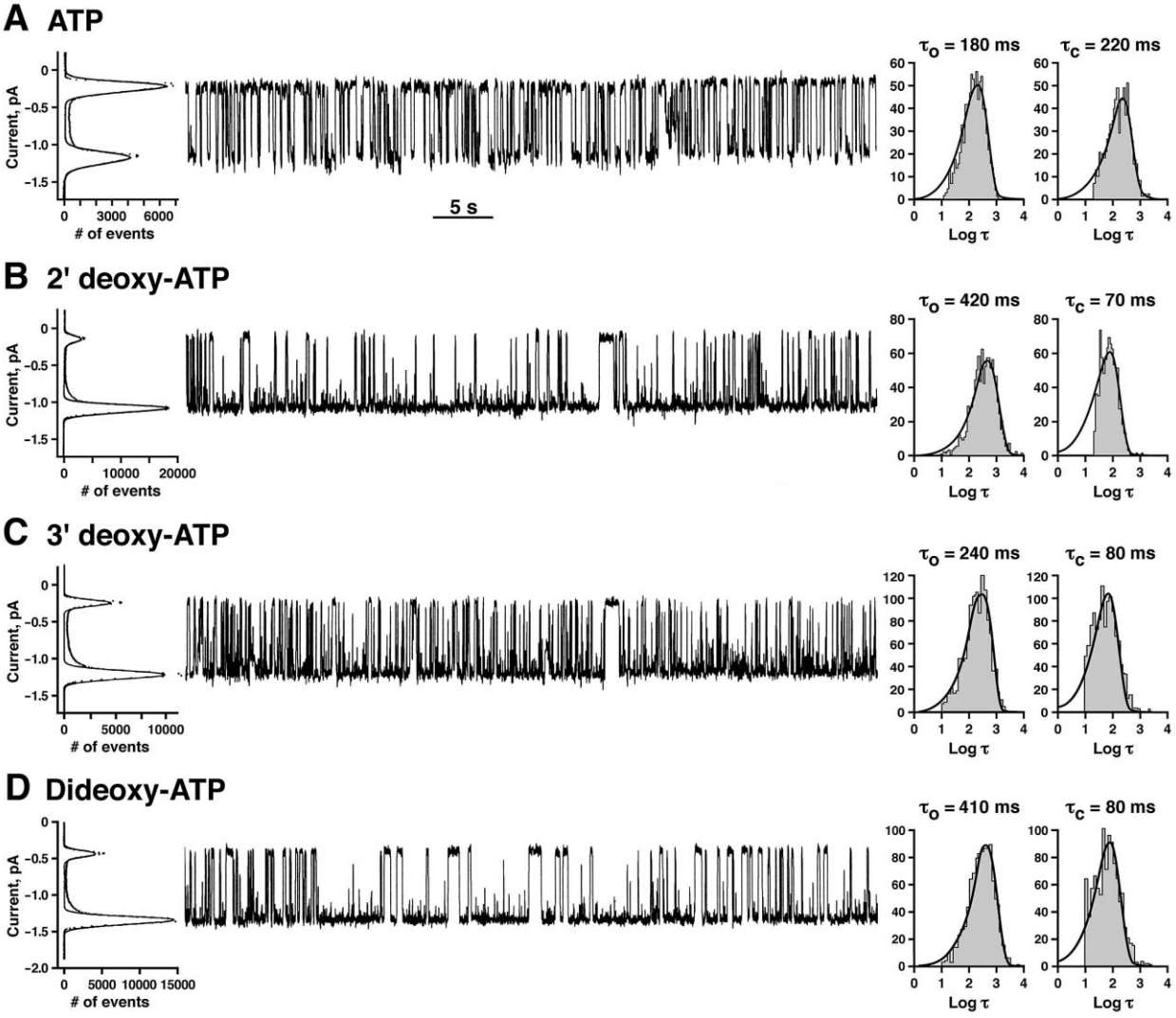

Fig. 1. dATP activation of CFTR chloride channels. Single channel records of the phosphorylated wild-type CFTR ion channel gated by 2 mM ATP (A), 2 mM 2′-dATP (B), 3′-dATP (C) and di-dATP (D) at 30°C. All points histograms are shown on the left. The areas under the peaks were used to calculate $P_o = 0.45$ (A), 0.82 (B), 0.71 (C) and 0.79 (D). Single channel conductances calculated as the distance between peaks on the all points histograms were invariant with the value of $\gamma = 12.4 \pm 0.3$ pS independent of the ligand. 1 min records are shown. Dwell-time histograms for closed and open states are shown on the right of these. The numerical values shown above the dwell-time histograms are the mean closed time and mean open times calculated for these particular experiments.

radioactivity in the resolved spots quantified by electronic autoradiography (Packard Instant Imager).

2.5. Materials

Phospholipids: 1-palmitoyl-2-oleoyl-*sn*-glycero-3-phosphoethanolamine and 1-palmitoyl-2-oleoyl-*sn*-glycero-3-phosphoserine were from Avanti Polar Lipids (Birmingham, AL, USA). The PKA catalytic subunit was from Promega (Madison, WI, USA). [α-^{32}P]ATP and [α-^{32}P]dATP were purchased from Amersham Pharmacia Biotech (Piscataway, NJ, USA). Alkaline phosphatase from bovine intestinal mucosa (type VII-L) and all other chemicals were from Sigma (St. Louis, MO, USA).

3. Results

3.1. dATP activates CFTR chloride channels more effectively than ATP

After phosphorylation by PKA, CFTR is effectively activated by 2 mM MgATP added to the *cis*-side of the bilayer as illustrated in Fig. 1A. Under symmetrical ionic conditions (300 mM Tris–HCl, pH 7.1) the wild-type CFTR ion channel has a conductance $\gamma = 12.3 \pm 0.6$ pS, a mean open time $\tau_o = 190 \pm 20$ ms, a mean closed time $\tau_c = 220 \pm 30$ ms and an open probability, $P_o = 0.45 \pm 0.05$. The results of an identical experiment where ATP was replaced by 2′-dATP are shown in Fig. 1B. The single channel conductance is seen to be unchanged but the gating kinetics are very significantly altered. Quantitatively, the mean open and closed times, shown above the dwell time histograms to the right of the tracings, indicate both an increase in τ_o and a decrease in τ_c with a resultant large increase in open probability ($P_o = 0.82$).

To clarify how important the 2′-position is, we tried to gate the wild-type CFTR ion channel with 2 mM 3′-dATP and didATP (Fig. 1C,D). The only difference noted was a two-fold decrease in mean open time with 3′-dATP compared with 2′-dATP. Thus the influence on the rate of the ion channel opening ($k_o = 1/\tau_c$) apparently does not depend on the position of the oxygen removed.

3.2. dATP is hydrolyzed by CFTR quite differently than ATP

ATP is bound and hydrolyzed by CFTR [12]. To directly compare the hydrolysis of the two nucleotides, wild-type CFTR was purified and reconstituted in liposomes. The purity of the wild-type CFTR is shown in Fig. 2C. In Fig. 2A the rates of ATP and dATP hydrolysis by purified CFTR are shown as a function of nucleoside triphosphate concentration.

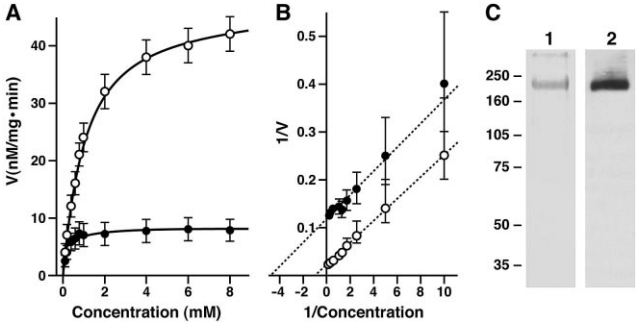

Fig. 2. Hydrolysis of ATP and dATP by purified CFTR. The rates of ATP (open circles) and dATP (solid circles) hydrolysis by purified wild-type CFTR as a function of substrate concentration are shown (A). The data shown are mean values ± S.D. of three experiments for ATP and two experiments for dATP. The Lineweaver–Burk graphs (B) were used to demonstrate the consistency of the experimental data with the Michaelis–Menten equation and the identity of V_{max}/K_M values for ATP and dATP. The numerical values are: $V_{max} = 47$ nmol/(mg min) and $K_M = 1.1$ mM for ATP (open circles) and $V_{max} = 8.5$ nmol/(mg min) and $K_M = 0.2$ mM for dATP (solid circles). SDS–PAGE of the purified CFTR protein assayed is shown in C: lane 1, Coomassie blue staining; lane 2, a Western blot probed with monoclonal antibody M3A7 [25].

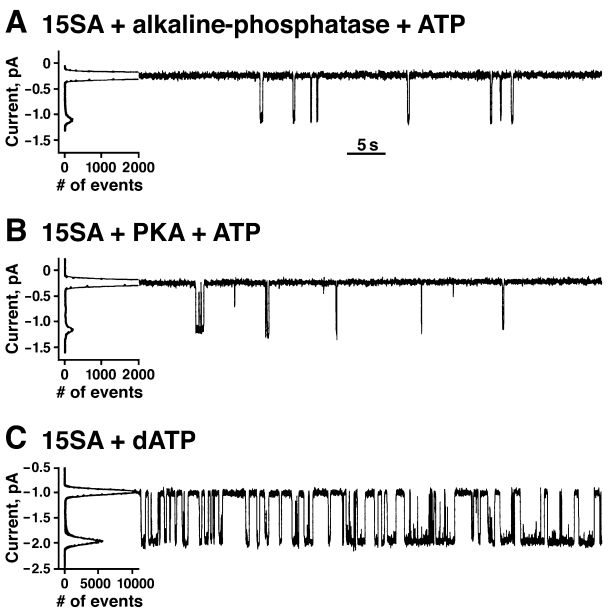

Fig. 3. dATP activates a PKA unresponsive CFTR variant. Single channel records of 15SA mutant gated by 2 mM MgATP (A, B) and 2 mM MgdATP (C) at 30°C are shown. Both alkaline phosphatase treated (A) and PKA phosphorylated (B) channels have the same single channel conductance, $\gamma = 12.4 \pm 0.3$ pS, and $P_o = 0.04$. With dATP (C), P_o increased to 0.38 with no change in single channel conductance, $\gamma = 12.4 \pm 0.3$ pS.

The Michaelis–Menten model was used to analyze the experimental data:

$$E + S \underset{k_2}{\overset{k_1}{\leftrightarrow}} ES \xrightarrow{k_3} E + P$$

where E is enzyme, S is substrate, ES is the enzyme–substrate complex, P is the product(s) and k_i are the rate constants. In the framework of this simple model the steady-state rate of the substrate transformation is:

$$v = k_3[ES] = V_{max}/(1 + K_M/[S]) \quad (1)$$

where $V_{max} = k_3 E_0$ and $K_M = (k_2 + k_3)/k_1$ is the Michaelis constant.

A Lineweaver–Burk plot (Fig. 2B) was used to demonstrate the consistency of the experimental points with the Michaelis–Menten equation and calculate the parameters V_{max} and K_M. The numerical values of $V_{max} = 47$ nmol/(mg min) and $K_M = 1.1$ mM for the ATP hydrolysis by CFTR are in good agreement with published data [12]. Both plots were prepared for non-phosphorylated wild-type CFTR. The value of the catalytic constant k_3 may be calculated as $k_3 = V_{max}/E_0 = 0.14\ s^{-1}$. Based on the fact that nucleotide binding domain 2 (NBD2) has much higher hydrolytic activity than NBD1 [13] and the assumption that hydrolysis at NBD2 may be sufficient to complete the gating cycle the minimal time for the gating cycle is $\tau_{cycle} = 1/k_3 = 7$ s. If hydrolysis at both NBDs occurred during the gating cycle the value of τ_{cycle}

would double to 14 s. The same experimental approach but with [α-^{32}P]dATP as a substrate, yields values of $V_{max} = 8.5$ nmol/(mg min), $K_M = 0.2$ mM, $k_3 = 0.025$ s^{-1} and $\tau_{cycle} = 1/k_3 = 40$ s (Fig. 2A,B). The slopes of both graphs in Fig. 2B are the same: $K_M/V_{max} = 1.1/47 = 0.2/8.5 \approx 0.023$ mM mg min/nmol.

3.3. Relation of dATP activation to CFTR phosphorylation

A prerequisite for MgATP-induced gating of wild-type CFTR is phosphorylation by PKA [14]. The actual mechanism of priming CFTR by PKA phosphorylation is complex and not fully understood [9,15]. We tested the influence of dATP on a variant in which all 15 serine residues that are phosphoryl group acceptors in the R-domain were mutagenized [9]. In this case where alanines replaced serines at all 15 phosphorylation sites (15SA) the channel is essentially unresponsive to PKA, exhibiting a $P_o = 0.04$ or less as illustrated in Fig. 3A,B regardless of phosphatase or kinase treatment. Due to the rare openings at this low level of activity it was impossible to prepare dwell-time histograms to calculate mean open and mean closed times. However, these could be roughly estimated as 200 ms and 5 s, respectively. Strikingly, however, when dATP is employed as substrate the channel becomes strongly active with a $P_o = 0.38$ (Fig. 3C). In this case it is possible to run dwell-time analysis and obtain values of $\tau_o = 370 \pm 40$ ms and $\tau_c = 540 \pm 50$ ms. This indicates that the action of the deoxynucleotide nearly completely circumvents or overcomes the requirement for R-domain phosphorylation.

To confirm that this could occur with even an unphosphorylated wild-type channel, membrane vesicles were treated with alkaline phosphatase to remove any residual phosphoryl groups from PKA sites. This renders the channels completely quiet in the presence of MgATP. No openings were observed during a total recording time of more than 5 h. Addition of PKA to the *cis*-chamber after this time resulted, after a period of 10–15 min, in channel activity with kinetics indistinguishable from the channel shown in Fig. 1A. However, replacement of MgATP with MgdATP generated robust channel activity without PKA treatment (Fig. 4). The single channel recording shown in Fig. 4A is from the alkaline phosphatase treated wild-type CFTR ion channel gated by 2 mM dATP. The single channel parameters are: $\gamma = 12.6$ pS, $P_o = 0.71$, $\tau_o = 450$ ms and $\tau_c = 140$ ms. The only difference between channels in Fig. 1B and Fig. 4A is the phosphorylation state. In both cases the single channel conductances do not change at all. The P_o values are similar (0.82 versus 0.71) and much higher than that of the wild-type CFTR ion channel phosphorylated by PKA with ATP as ligand (Fig. 1A). As was the case without phosphatase treatment, the exact position on the pentose ring of the removed oxygen is apparently not crucial. In spite of some differences in mean closed times the non-phosphorylated wild-type CFTR is gated succesfully by 3′-dATP and di-dATP also (Fig. 4B,C). Thus, CFTR channel gating can be driven by MgdATP in the complete absence of phosphorylation by PKA which is strictly required for the gating driven by MgATP.

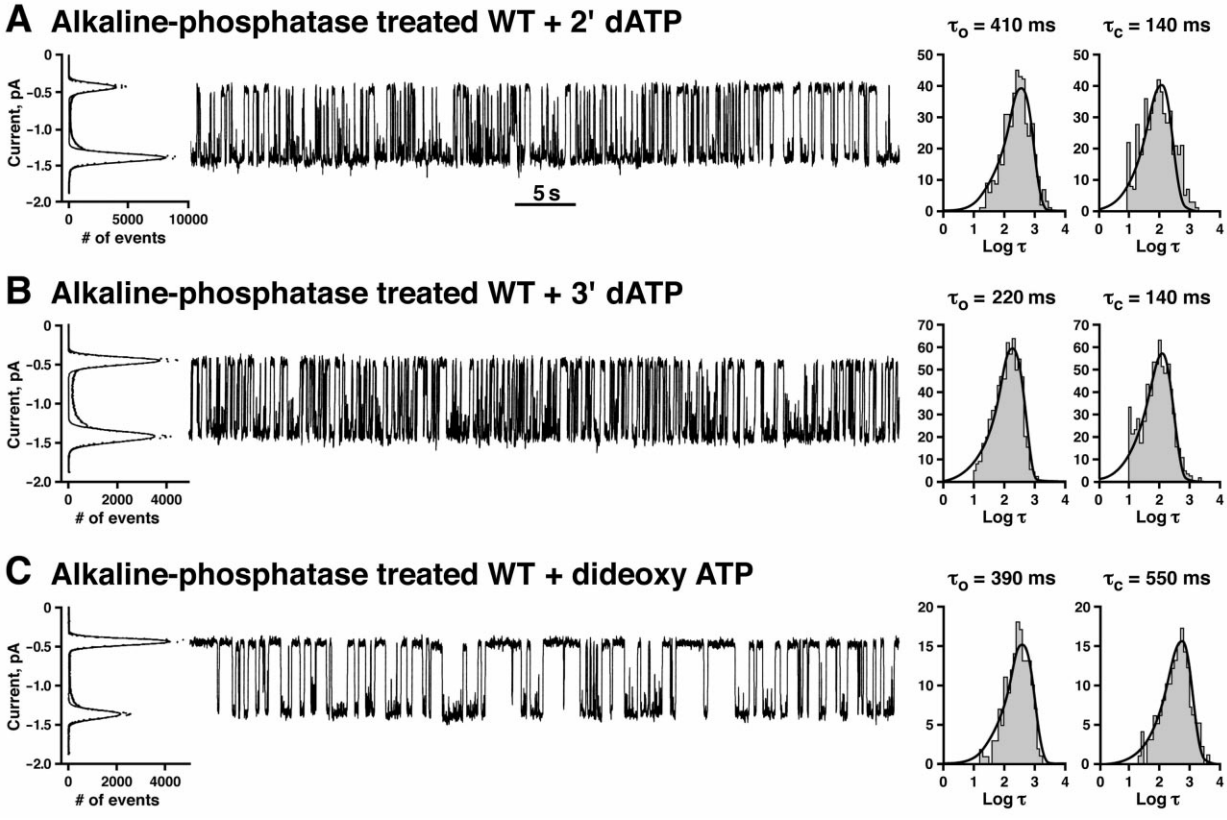

Fig. 4. dATP activates dephosphorylated wild-type CFTR. After alkaline phosphatase treatment of the wild-type CFTR, no single channel openings were recorded with 2 mM MgATP^{2-}. Channel activity may be restored by addition of 100 U/ml PKA to the *cis*-compartment (not shown) or by replacement of 2 mM ATP with 2 mM 2′-dATP (A), 3′-dATP (B) or di-dATP (C). The single channel conductance, $\gamma = 12.4 \pm 0.3$ pS, was calculated from the all points histograms shown on the left of the records. Dwell-time histograms for the open time and closed time are shown on the right. Mean open and mean closed times are shown above the dwell-time histograms.

4. Discussion

We have examined an aspect of nucleotide structure that has received no previous attention in studies of these molecules as ligands that gate the CFTR ion channel. With dATP substituted for ATP the mean open time (τ_o) increased. Together with a three-fold decrease in mean closed time (τ_c) the overall P_o increases about two-fold. This demonstrates that performance of the wild-type CFTR ion channel was improved when dATP replaced ATP and this improvement is a result of both better stability of the open channel structure ($k_c = 1/\tau_o$) and acceleration of channel openings ($k_o = 1/\tau_c$). Based on the data shown in Fig. 1 we can conclude that mean open time is sensitive to the position from which oxygen is removed from the pentose ring. Conversely, the mean closed time is not sensitive and any oxygen removal from either position in the pentose ring accelerates channel opening about three times.

The large difference in CFTR's ability to hydrolyze dATP and ATP (see Fig. 2) together with the strong effect on channel gating provides a new opportunity to evaluate the relationship between the two functions of the protein, i.e. between ion channel gating and ligand(s) hydrolysis in a direct experiment. If the two are tightly coupled as in a model where hydrolysis drives gating their kinetics should be very similar.

However, the total gating cycle time for the wild-type CFTR ion channel gated by ATP (Fig. 1) $\tau_{cycle} = \tau_o + \tau_c = 0.4$ s which is about 20-fold less than the minimal time estimated for the ATP hydrolytic cycle ($\tau_{cycle\,min} = 7$ s). This discrepancy could be due to a low yield ($\sim 5\%$) of active CFTR on purification and reconstitution. If the sidedness of the protein orientation in liposomes is random this estimate would be increased to $\sim 10\%$. An alternative explanation is that there are multiple gating cycles for each hydrolytic event [16,17]. By using two different substrates we are able to compare ratios of their kinetic parameters independent of the level of recovery of functional protein during purification. For substrate concentrations close to the saturation range the value of $\tau_{cycle}^{ATP}/\tau_{cycle}^{dATP} = V_{max}^{dATP}/V_{max}^{ATP} = 0.18$ does not match well with $\tau_{cycle}^{ATP}/\tau_{cycle}^{dATP} = (\tau_o^{ATP} + \tau_c^{ATP})/(\tau_o^{dATP} + \tau_c^{dATP}) = 0.73$. This suggests a complex relationship between ion channel gating and nucleotide triphosphate hydrolysis. Since the K_M and V_{max} values for ATP hydrolysis with our present purification and reconstitution agree very well with those obtained by an entirely different preparation where the yield of functional protein was high [18], it is unlikely that this factor contributes greatly to differences in catalytic and gating rates with ATP. In any case utilizing the ratios of values with ATP and dATP avoids the need for accurate estimates of functional recovery in our mechanistic speculations.

According to the rate law, the value of V_{max}/K_M (1/slope on the graph in Fig. 2B) is the apparent first-order rate constant at low substrate concentration ($[S] \ll K_M$). Our experimental data show this value remains constant with substitution of dATP for ATP (lines are parallel in Fig. 2B). Let us consider factors that determine the value of $V_{max}/K_M = k_1 k_3 E_o/(k_2 + k_3)$. For molecules with a minor difference in structure like ATP and dATP we can reasonably suppose the same restrictions of diffusion to the binding sites ($k_{1\,ATP} = k_{1\,dATP}$). At very low substrate concentrations ($[S] \ll K_M$) we can expect the same equilibrium distribution among possible conformational states of the enzyme independent of the type of ligand ($E_o \approx [E] \gg [ES]$). The most interesting factor defining the V_{max}/K_M value is the so-called reaction 'yield' or $k_3/(k_2+k_3)$. It represents the proportion of the first collision complex between enzyme and substrate which goes on to produce products, as opposed to dissociating back to E and S [19]. It includes all steps following substrate addition up to and including the first irreversible step, which usually is release of the first product [19]. With the assumptions mentioned above, the constant value of V_{max}/K_M requires the same value of the 'yield' for both substrates. This leads us to the conclusion that any differences in the rates of hydrolysis between ATP and dATP take place due to the differences in the steps following the first irreversible step. It may be the release of any further products and/or relaxation of the enzyme structure to the initial ligand-free configuration but not the cleavage of the chemical bond itself. On this basis we can further conclude that in the millimolar range of substrate concentration one of these former two possibilities is the rate-limiting step in the CFTR hydrolytic cycle rather than nucleotide triphosphate binding and hydrolysis. This is in good agreement with our previous conclusion that channel closings occur as a result of dissociation of the hydrolysis products or of the ligand itself [6,10].

The most striking aspect of the action of dATP on CFTR is its apparent ability to circumvent the need for phosphorylation of the R-domain by PKA. Interpretation of how this may occur is somewhat hindered by the lack of understanding of how this phosphorylation normally enables the induction of gating transitions by nucleotide interactions at the NBDs [20]. The role of R-domain phosphorylation on channel activation has been shown to be complex involving both the relief of an inhibitory effect of unphosphorylated R-domain and an active stimulatory effect of the phosphorylated domain [21,22]. The mechanistic implications of the results are not immediately obvious. This reflects both the facts that even in the NBDs of other adenine nucleotide binding cassette proteins where three-dimensional structures have been solved there are quite varied or ill-defined interactions with the pentose ring [23] and that the regulation of CFTR gating in general remains poorly understood [24].

Acknowledgements: This work was supported by DK51619 and the Cystic Fibrosis Foundation.

References

[1] Yount, R.G. (1975) Adv. Enzymol. Relat. Areas Mol. Biol. 43, 1–56.
[2] Freist, W. (1988) Angew. Chem. Int. Ed. Engl. 27, 773–788.
[3] Anderson, M.P., Berger, H.A., Rich, D.P., Gregory, R.J., Smith, A.E. and Welsh, M.J. (1991) Cell 67, 775–784.
[4] Travis, S.M., Carson, M.R., Ries, D.R. and Welsh, M.J. (1993) J. Biol. Chem. 268, 15336–15339.
[5] Quinton, P.M. and Reddy, M.M. (1992) Nature 360, 79–81.
[6] Aleksandrov, A.A., Chang, X., Aleksandrov, L. and Riordan, J.R. (2000) J. Physiol. 528 (Part 2), 259–265.
[7] Berger, A.L. and Welsh, M.J. (2000) J. Biol. Chem. 275, 29407–29412.
[8] Berger, A.L. and Welsh, M.J. (2002) in: Biophysical Society 46th Annual Meeting, Vol. 82, p. 240a, San Francisco, CA.
[9] Seibert, F.S., Chang, X.B., Aleksandrov, A.A., Clarke, D.M., Hanrahan, J.W. and Riordan, J.R. (1999) Biochim. Biophys. Acta 1461, 275–283.
[10] Aleksandrov, A.A. and Riordan, J.R. (1998) FEBS Lett. 431, 97–101.
[11] Chang, X.-B., Tabcharani, J.A., Hou, Y.-X., Jensen, T.J., Kart-

ner, N., Alon, N., Hanrahan, J.W. and Riordan, J.R. (1993) J. Biol. Chem. 268, 11304–11311.
[12] Li, C. et al. (1996) J. Biol. Chem. 271, 28463–28468.
[13] Aleksandrov, L., Aleksandrov, A.A., Chang, X.-B. and Riordan, J.R. (2002) J. Biol. Chem. Papers, in press published on Feb. 22, 2002 as manuscript M111713200.
[14] Tabcharani, J.A., Chang, X.-B., Riordan, J.R. and Hanrahan, J.W. (1991) Nature 352, 628–631.
[15] Gadsby, D.C. and Nairn, A.C. (1999) Physiol. Rev. 79, S77–S107.
[16] Ramjeesingh, M., Li, C., Garami, E., Huan, L.J., Galley, K., Wang, Y. and Bear, C.E. (1999) Biochemistry 38, 1463–1468.
[17] Weinreich, F., Riordan, J.R. and Nagel, G. (1999) J. Gen. Physiol. 114, 55–70.
[18] Bear, C.E., Li, C., Kartner, N., Bridges, R.J., Jensen, T.J., Ramjeesingh, M. and Riordan, J.R. (1992) Cell 68, 809–818.
[19] Cleland, W.W. (1975) Acc. Chem. Res. 8, 145–151.
[20] Hanrahan, J.H., Gentzsch, M. and Riordan, J.R. (2002) in: ABC Proteins from Bacteria to Man (Holland, B., Cole, S.P.C., Kuchler, K. and Higgins, C.F., Eds.), Academic Press, London, in press.
[21] Winter, M.C. and Welsh, M.J. (1997) Nature 389, 294–296.
[22] Ostedgaard, L.S., Baldursson, O. and Welsh, M.J. (2001) J. Biol. Chem. 276, 7689–7692.
[23] Yuan, Y.R., Blecker, S., Martsinkevich, O., Millen, L., Thomas, P.J. and Hunt, J.F. (2001) J. Biol. Chem. 276, 32313–32321.
[24] Zou, X. and Hwang, T.C. (2001) Biochemistry 40, 5579–5586.
[25] Kartner, N., Augustinas, O., Jensen, T.J., Naismith, A.L. and Riordan, J.R. (1992) Nat. Genet. 1, 321–327.